Molecular Weight Effects on the Phase Diagram of Polystyrene–Poly(vinyl methyl ether) Blends†

J. M. Ubrich, F. Ben Cheikh Larbi, J. L. Halary,* and L. Monnerie

Laboratoire de Physicochimie Structurale et Macromoléculaire, Ecole Supérieure de Physique et de Chimie Industrielles de la Ville de Paris, F-75231 Paris Cedex 05, France

B. J. Bauer and C. C. Han

Polymer Division, National Bureau of Standards, Gaithersburg, Maryland 20899.
Received June 27, 1985

ABSTRACT: Fluorescence emission of labeled polystyrene is employed to reexamine the lower critical solution temperature phase diagram of the system polystyrene (PS)–poly(vinyl methyl ether) (PVME) over a large range of molecular weights. The influence of polymer chain length is investigated by using a variety of PS's and PVME's having molecular weights ranging from 20 400 to 1 660 000 and from 45 000 to 1 330 000, respectively. Fluorescence measurements are shown to be suitable for the determination of the coexistence curve, even in the case of the largest molecular weights, for which the phase separation process develops very slowly. Particular attention is paid to a series of blends in which the molecular weight of one component is kept constant, whereas that, $\bar{M}_w(i)$, of the other one varies. In agreement with Scott's treatment of polymer mixtures, a linear relationship is found between $(\bar{M}_w(i))^{1/2}$ and $(w_{min}(i))^{-1}$, the reverse of the composition at which the boundary temperature exhibits a minimum. However, the effects of PS and PVME chain length may be less symmetrical than expected from reference volume current ideas, owing to the solvating capability of the shortest PVME chains.

Introduction

This report forms part of a series of studies on the application of fluorescence emission of labeled polystyrene to the analysis of thermally induced phase separation phenomena in polystyrene (PS)–poly(vinyl methyl ether) (PVME) blends. As shown in a previous work,[1] this new method is based on a particular phenomenon. Some static quenching of the fluorescence emission of anthracene-labeled polystyrene (PS*) by PVME occurs in the miscible blends but tends to cease as phase separation develops. This method permits detection of the earliest stages of phase separation and is suitable for the determination of both the binodal and spinodal curves of the phase diagram. Recently, this method has been applied to the study of the dependence of the phase diagram of PS–PVME on whether the polystyrene is hydrogenous or deuterated.[2] In this paper, we go back on the phase diagram of binary blends of hydrogenous PS–PVME and investigate the influence of both PS and PVME chain length over a large range of molecular weights.

The first objective of this work is to verify if the fluorescence method, which was developed earlier[1] for the case of a polydisperse PVME ($\bar{M}_w$ = 99 000) blended with various narrow distribution PS's (in the $\bar{M}_w$ range 20 400–233 000), is suitable for the determination of the phase diagram when the speed of the phase separation process is slowed down. The second objective is to analyze the location of the coexistence curve, and chiefly of its minimum, as a function of the chain length of the two polymers. In so doing, we will reexamine some previous findings[1,3,4] deduced from data relative to a restricted range of molecular weights.

Experimental Section

Materials. The origin and molecular weight characteristics of the polymer samples under study are given in Table I. Most of them are commercially available. The low molecular weight PVME V45 was isolated from a commercial V99 sample by preparative gel permeation chromatography experiments. The high molecular weight PVME's were synthesized at the National Bureau of Standards and do not contain any stabilizing additive. The labeled PS (PS*), including one anthracenic group in the middle of the chains, was the same as that used in previous studies.[1,2] Prior to blending, the materials were dried for 24 h at 60 °C under reduced pressure with a residual atmosphere of nitrogen.

Table I
Polymer Origin and Characteristics

polymer	sample	origin	$\bar{M}_n$	$\bar{M}_w$	$\bar{M}_w/\bar{M}_n$
PS	S20	Pressure Chemical Co.	19 300	20 400	1.06
	S35	Polymer Labs Ltd.	34 000	35 700	1.05
	S67	this lab (Paris)	62 000	67 000	1.08
	S106	Pressure Chemical Co.	100 000	106 000	1.06
	S233	Polysciences Inc.	220 000	233 000	1.06
	S381	this lab (Paris)	307 000	381 000	1.24
	S600	Pressure Chemical Co.	545 000	600 000	1.10
	S759	EAHP (Strasbourg)	660 000	759 000	1.15
	S1660	EAHP (Strasbourg)	1 300 000	1 660 000	1.28
PVME	V45	CNRS (Paris)	22 000	45 000	2.05
	V99	Scientific Polymer Products	46 500	99 000	2.12
	V388	NBS	229 000	388 000	1.69
	V633	NBS	370 000	633 000	1.71
	V1330	NBS	547 000	1 330 000	2.47

Blend Preparation. Benzene solutions (10%) of PVME/PS/PS* were prepared by varying the weight ratio of PVME/PS in the range 0.1–0.9 and fixing the PS* content in such a way to label the polymer mixture with around 6 ppm of anthracenic groups. Films were cast on glass plates and then dried in an oven under nitrogen, first at room temperature for 24 h, next at 60 °C for 24 h, and finally under vacuum until complete removal of the solvent had occurred.

Fluorescence Measurements. Measurements were carried out under continuous illumination by using a fluorescence microscope with excitation and fluorescence emission wavelengths around 365 and 440 nm, respectively. As shown previously,[1] the immiscibility threshold is detected in the form of an upturn in fluorescence intensity. Some experiments were performed in a Mettler hot stage under continuous heating at a speed ranging from 0.2 to 16 °C·min^{-1}; others were carried out under isothermal

† Dedicated to Dr. Pierre Thirion on the occasion of his retirement in 1985.

0024-9297/86/2219-0810$01.50/0

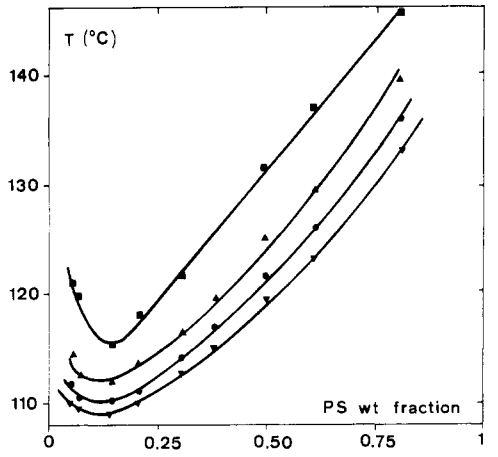

Figure 1. Influence of composition and heating rate on detected phase separation temperatures for the system V99–S600. Heating rate (°C·min^{-1}): (▼) 0.2; (●) 1; (▲) 5; (■) 16.

conditions by waiting at least 30 min for any change in fluorescence intensity.

Results and Discussion

Blends of PVME V99 with High Molecular Weight PS's. The temperature at which the phase separation is detected depends on the heating rate of the samples (series S381–S1660, in Table I) all over the composition range of the blends, as illustrated in Figure 1 for the mixture V99–S600. One may notice that the heating rate influence is significant even around the minimum of the phase diagram. This feature contrasts with our previous data[1] on lower molecular weight PS's (series S20–S106 in Table I), which do not reveal any effect of this experimental parameter around the minimum of the curves. The situation encountered with S233[1] may be considered a posteriori as being intermediate.

As a general rule, data obtained from experiments carried out at 0.2 °C·min^{-1} can be regarded as providing a reasonable approximation of the equilibrium boundary. Indeed, 30-min isothermal experiments performed 1 °C below the experimental curve did not lead to any change in fluorescence intensity, confirming the absence of phase separation in such conditions. The one exception deals with the blend V99–S1660, for which the heating rate of 0.2 °C·min^{-1} itself is too fast compared with the phase separation process. In this case, isothermal experiments are the unique route toward binodal determination.

Actually, the above given results are not inconsistent with our previous findings,[1] they just show from which molecular weight the applied heating rate matches the speed of phase separation. In order to support this conclusion, let us concentrate on data relative to the composition w_{min} of the minimum of the phase diagrams and characterize the extent of the heating rate effect by the quantity $\Delta T = T_{16} - T_{min}$, the difference between the temperatures at which the phase separation is detected in experiments at 16 °C·min^{-1} and under isothermal conditions, respectively. Because the only mechanism that is expected to occur in the vicinity of w_{min} is spinodal decomposition, the quantity ΔT is related to the speed of this process. As long as spinodal decomposition occurs fast enough with respect to the heating rate, the temperature at which phase separation is detected coincides with T_{min}. On the other hand, when this speed is drastically slowed down owing to the molecular weight of the materials, the temperature at which the increase in fluorescence is observed is higher than T_{min}, and ΔT varies as the detection time lag. The molecular weight dependence of ΔT (and, as a general rule, of all the quantities under consideration in this paper) is analyzed on the basis of weight-average molecular weights $\bar{M}_w$, in accordance with the current treatment of polydisperse systems.[5] As shown in Figure 2, ΔT is zero for a PS weight-average molecular weight $\bar{M}_w$(PS) below 70 000 and then increases linearly with $\bar{M}_w$(PS). This result is consistent with the molecular weight dependence of the quantity $-\tau_q^{-1}$, defined by Pincus[6] as the growth rate of the dominant concentration fluctuation; this quantity should decrease when the molecular weight increases, as qualitatively observed by Gelles and Frank.[7]

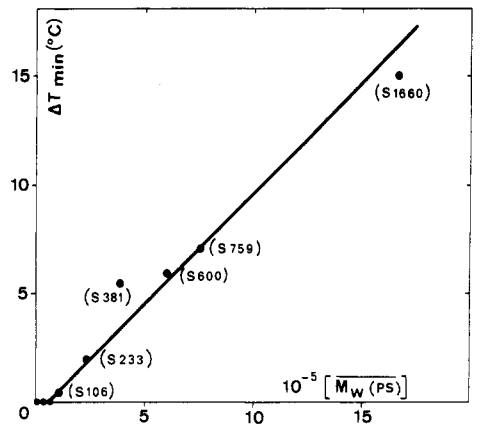

Figure 2. Variation of ΔT with PS molecular weight for PS–V99 mixtures.

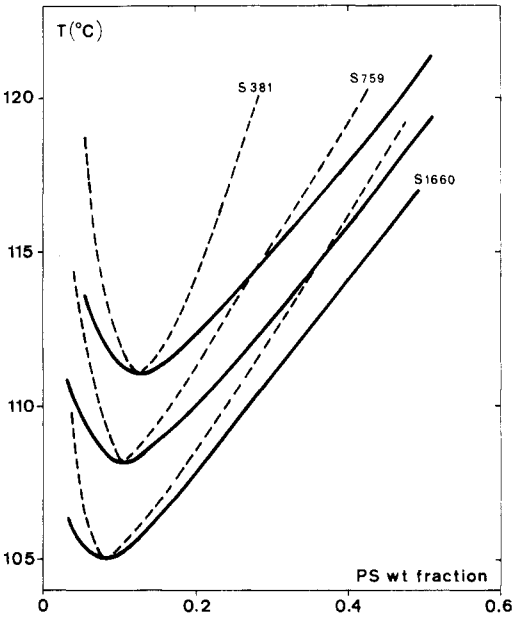

Figure 3. Sketch of experimental binodals (solid curves) and estimated spinodals (dashed curves) for mixtures of V99–high molecular weight PS.

From a practical viewpoint, existence of large ΔT values stands in the way of a precise determination of the spinodal curve, insofar as it is distinguished from the binodal (in our method), thanks to heating rate effects. At best, the spinodal curve can be estimated by shifting the experimental curve at 16 °C·min^{-1} to lower temperature by the amount ΔT. This procedure assumes that ΔT is independent of the blend composition. However, this cannot be experimentally verified. Evolution of the phase diagrams as a function of $\bar{M}_w$(PS) is sketched in Figure 3 for samples S381, S759, and S1660.

Let us focus now on the minima of the boundary curves, characterized by a PS weight fraction w_{min} and a tem-

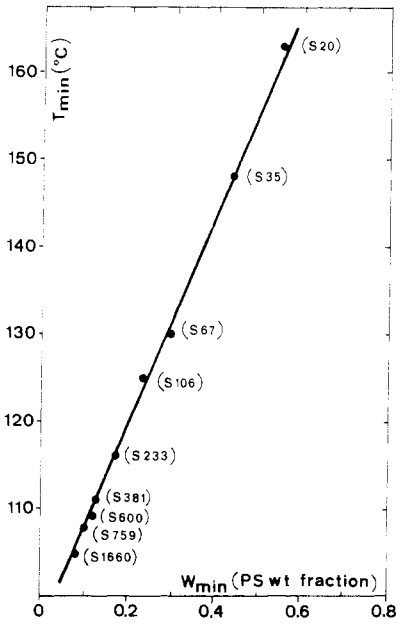

Figure 4. Plot of T_{min} vs. w_{min} for PS–V99 mixtures.

Table II
Values of $(T_{min})_\infty$ As Determined from Least-Squares Curve Fitting

	$(T_{min})_\infty$ deduced from plots of T_{min}	
series of blends	against $[\bar{M}_w(i)]^{-1/2}$	against $w_{min}(i)$
PVME V99–PS	96.7	96.3
PS S106–PVME	97.0	94.3
PVME V388–PS	99.1	98.8

perature T_{min}. As shown in Figure 4, the experimental data confirm the validity of the linear relationship between T_{min} and w_{min}, previously evidenced[1] over a more restricted range of $\bar{M}_w$(PS). On the contrary, the molecular weight dependence of T_{min}[1] has to be reexamined. Indeed, the linear variation of T_{min} with the inverse of $\bar{M}_w$(PS) is proving inconsistent with data relative to the largest values of $\bar{M}_w$(PS) (Figure 5a). In fact, the best way to fit the experimental data over the entire $\bar{M}_w$(PS) range (20 400–1 660 000) is to plot T_{min} vs. $(\bar{M}_w(PS))^{-1/2}$. As shown in Figure 5b, a straight line is obtained. Mean squares analysis of this curve provides us with its analytic characteristics; the value of the intercept with the y axis, the so-called $(T_{min})_\infty$, is of particular interest because it represents the minimum temperature at which phase separation should occur in the case of a blend of PVME V99–PS of infinite molecular weight. This quantity $(T_{min})_\infty$ may be also determined as the intercept with the y axis of the curve T_{min} vs. w_{min} (Figure 4), since, if $\bar{M}_w$(PS) tends to infinity, then w_{min} tends to zero. An excellent agreement is found between the two methods of calculation, as shown in Table II.

Blends of PS S106 with Different PVME's. The purpose of this section is to provide us with information comparable to those above gained by varying $\bar{M}_w$(PS) at constant $\bar{M}_w$(PVME). An additional obstacle arises from PVME polydispersity which differs markedly from one sample to the other (Table I). However, one may shake off this difficulty by agreeing to larger confidence ranges as an account of polydispersity effects.

As above, the temperature at which the phase separation is detected from fluorescence measurements depends on both the blend composition and the heating rate. This behavior is illustrated in Figure 6 for the mixture S106–V388. Again, experiments performed at 0.2 °C·min^{-1} lead to the same temperatures (within the experimental error)

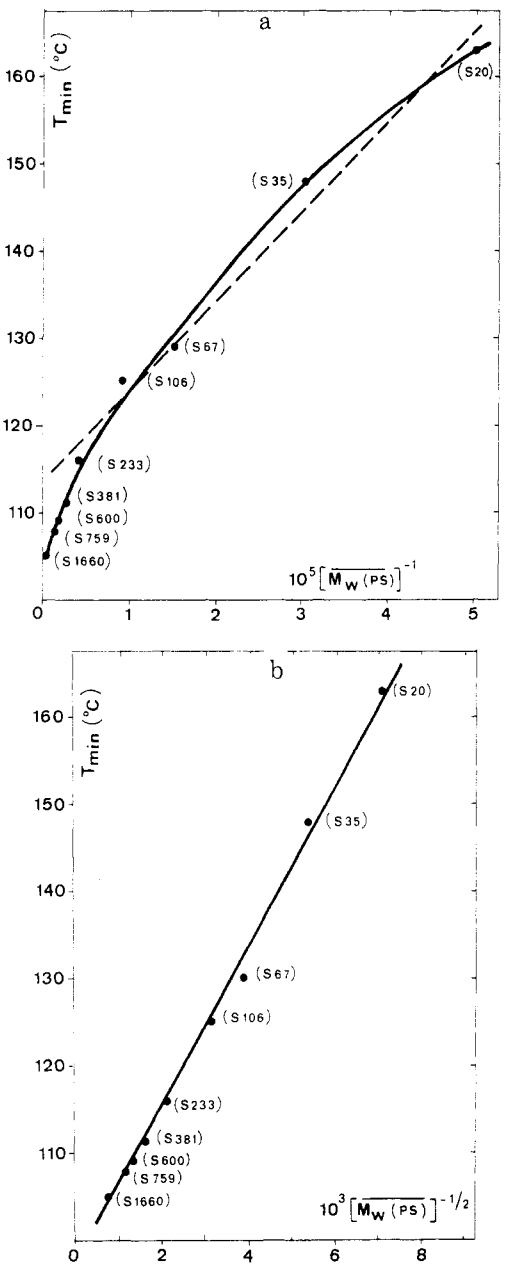

Figure 5. Search for the T_{min} dependence on PS molecular weight in PS–V99 mixtures: (a) plot of T_{min} vs. $(\bar{M}_w(PS))^{-1}$; (b) plot of T_{min} vs. $(\bar{M}_w(PS))^{-1/2}$.

as isothermal measurements, whereas experiments at 16 °C·min^{-1} are characterized by a molecular weight dependent heating rate effect ΔT. This dependence is schematized in Figure 7 in the form of a linear relation, by analogy to the above given data (Figure 2). Evolution of phase diagrams as a function of $\bar{M}_w$(PVME) is shown in Figure 8, in consideration of the same assumptions as in Figure 3 about the location of spinodal curves. The characteristics T_{min} and w_{min} obey a similar set of linear relationships as previously, i.e., (i) between T_{min} and $(\bar{M}_w(PVME))^{-1/2}$, and (ii) between T_{min} and $w_{min}(PVME) = (1 - w_{min})$ (w_{min}, indeed, means a PS weight fraction). $(T_{min})_\infty$, as determined from least-squares curve fitting (Table II), represents now the minimum temperature at which phase separation should occur in the case of a blend of PS S106–PVME of infinite molecular weight.

Blends of PVME V388 with Different PS's. A study of these additional systems was undertaken with the aim to confirm the above-given results. Unfortunately, phase separation develops excessively slowly in the blends

Table III
Analysis of Phase Diagram Minima for the Different Blends under Study

blend components	T_{min}, °C	w_{min}	$[(\phi_{PS})_{min}]^{-1}$	x_{PVME}	x_{PS}	$(x_{PS}/x_{PVME})^{1/2}$	fit factor α
V99–S20	163	0.55	1.85	1707	340	0.45	1.4–2.5
V99–S35	148	0.50	2.04	1707	594	0.59	1.4–2.3
V99–S67	130	0.29	3.54	1707	1115	0.81	2.6–3.8
V99–S106	125	0.235	4.37	1707	1764	1.03	2.8–4.0
V99–S233	116	0.175	5.88	1707	3878	1.51	2.7–3.9
V99–S381	112	0.125	8.25	1707	6341	1.93	3.2–4.4
V99–S600	109	0.12	8.60	1707	9985	2.42	2.7–3.7
V99–S759	108	0.11	9.38	1707	12631	2.72	2.6–3.6
V99–S1660	105	0.08	12.91	1707	27626	4.02	2.5–3.5
V45–S106	131	0.20	5.14	776	1764	1.51	2.3–3.3
V388–S106	109	0.67	1.51	6690	1764	0.51	0.7–1.4
V633–S106	106	0.72	1.40	10914	1764	0.40	0.7–1.5
V1330–S106	103	0.80	1.26	22931	1764	0.28	0.5–1.5
V388–S233	106	0.40	2.55	6690	3878	0.76	1.6–2.5
V388–S600	103	0.30	3.42	6690	9985	1.22	1.6–2.4

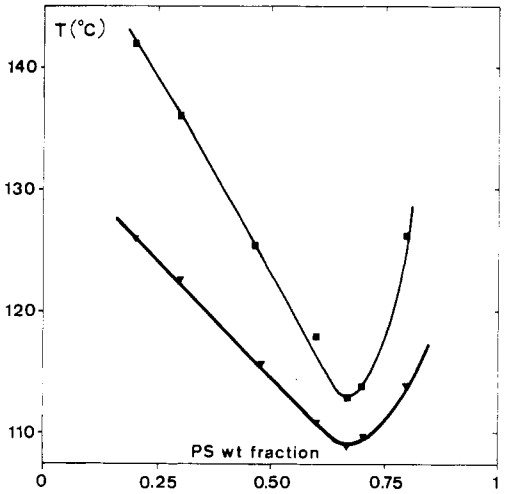

Figure 6. Influence of composition and heating rate on detected phase separation temperatures for the system V388–S106. Heating rate (°C·min^{-1}): (▼) 0.2; (■) 16.

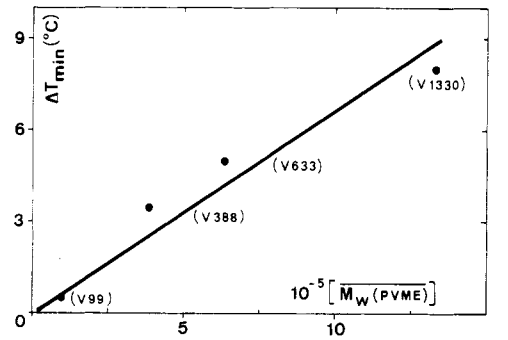

Figure 7. Variations of ΔT with PVME molecular weight for PVME–S106 mixtures.

V388–S233 and V388–S600 because of the large molecular weights of both components. As a consequence, isothermal experiments only are suitable and phase diagram determinations are less accurate than usual because fluorescence signal fluctuations over long-lived experiments end in matching the expected changes in intensity. However, T_{min} and w_{min} remain attainable with confidence (Table III) and continue to satisfy linear relationships between T_{min} and $(\bar{M}_w(PS))^{-1/2}$ and between T_{min} and w_{min} as well. Additionally, the intercepts with the y axis provide us with values of $(T_{min})_\infty$ (Table II).

General Discussion. A question remains open to discussion: why do the empirical relations between T_{min} and $(\bar{M}_w(i))^{-1/2}$ and between T_{min} and $w_{min}(i)$ hold? Since T_{min} varies linearly as a function of both $w_{min}(i)$ and

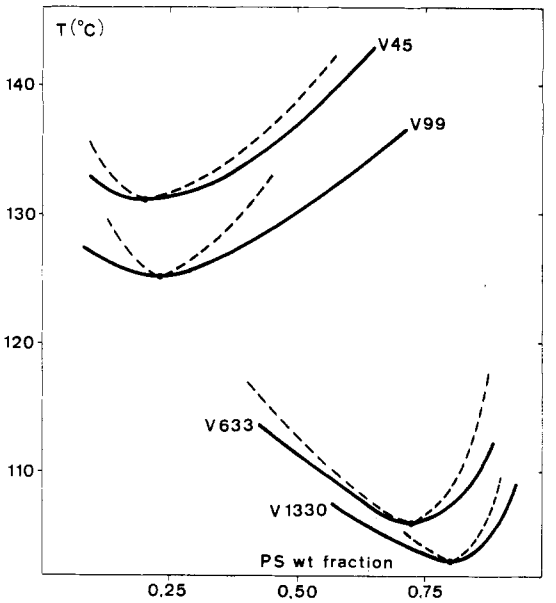

Figure 8. Sketch of experimental binodals (solid curves) and estimated spinodals (dashed curves) for mixtures of PVME–S106.

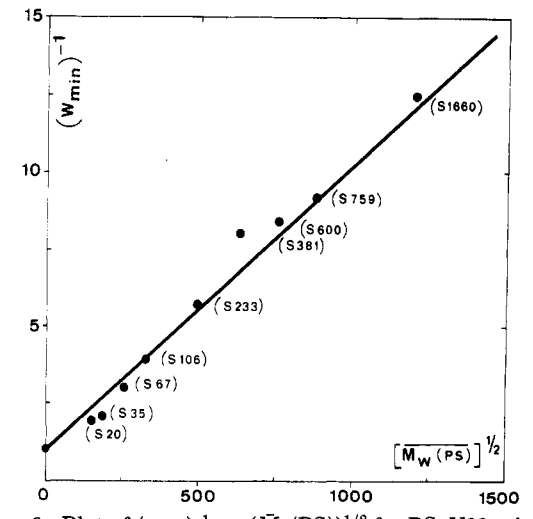

Figure 9. Plot of $(w_{min})^{-1}$ vs. $(\bar{M}_w(PS))^{1/2}$ for PS–V99 mixtures.

$(\bar{M}_w(i))^{-1/2}$, one may conclude the existence of a linear relation between $(w_{min}(i))^{-1}$ and $(\bar{M}_w(i))^{1/2}$. This is illustrated in Figure 9 in the case of the series PVME V99–PS, for which the experimental data are the most numerous. It is worth noting that this relation is consistent with one of the critical conditions that are satisfied in a mixture of two isomolecular polymers A and B. According to Scott,[8]

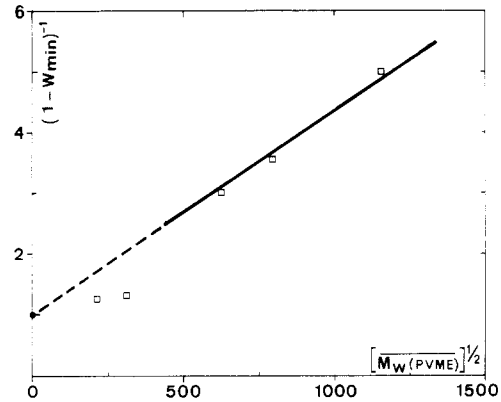

Figure 10. Plot of $(1 - w_{min})^{-1}$ vs. $(\bar{M}_w(\text{PVME}))^{1/2}$ for PVME–S106 mixtures.

the critical volume fraction of polymer A, $(\phi_A)_{cr}$, obeys the equation

$$(\phi_A)_{cr} = (x_B)^{1/2}/[(x_A)^{1/2} + (x_B)^{1/2}] \quad (1)$$

In this equation, x_A and x_B are the degree of polymerization of polymer A and polymer B in terms of the reference volume, V_r, respectively, and V_r is taken as close to the molar volume of the smallest polymer repeat unit as possible. In our experimental conditions, x_B, which deals here with PVME, is a constant since the same material (V99) is used in all blends under consideration and x_A is proportional to $\bar{M}_w$(PS). In addition, the polymer volume fraction and the polymer weight fraction are closely related quantities since both polymers have a comparable density: 1.011 and 0.096 at 398 K[9] for PS and PVME, respectively. Consequently, eq 1 may be rewritten in the form

$$(\phi_{PS})_{cr}^{-1} = 1 + (x_{PS}/x_{PVME})^{1/2} \quad (2)$$

and

$$(w_{min})^{-1} = 1 + k(\bar{M}_w(\text{PS}))^{1/2} \quad (3)$$

where k is a constant. As previously indicated, the weight-average molecular weight $\bar{M}_w$(PS) has been used in eq 3, in accordance with the current treatment of polydisperse systems.[5] However, one may notice that the number-average molecular weight should be suitable as well in eq 3 inasmuch as the different PS's used in the experiments have a similar polydispersity. As shown in Figure 9, the experimental data fit correctly eq 3, in consideration of both the proportionality between $(w_{min})^{-1}$ and $\bar{M}_w(\text{PS})^{1/2}$ and also the experimental value of the intercept with the y axis (0.94 as deduced from a least-squares analysis of the experimental data).

Although the experimental data available are less numerous in the case of the series PS S106–PVME the same analysis remains valid and the experimental data (Figure 10) are consistent with an equation of the form

$$(1 - w_{min})^{-1} = 1 + k(\bar{M}_w(\text{PVME}))^{1/2} \quad (4)$$

These conclusions mean, in contrast with McMaster's theoretical predictions,[5] that the polydispersity of one of the blend components does not oblige the critical point to move far away from the minimum of the temperature–composition diagram. Such a finding, which might appear as being unexpected, is actually corroborated by the shape of the phase diagrams, especially when both the binodal and spinodal are unambiguously determined (blends V99–low molecular weight PS[1] or blends V99–deuterated PS,[2a] for example). Binodal and spinodal, indeed, exhibit a common tangent at the extremum of the phase diagram but nowhere else.

One may dwell on the fact that the study of a series of blends in which the molecular weight of one component is kept constant whereas that of the other one varies is favorable, because this allows us to put the general equation 1 in the form

$$(w_{min}(\text{i}))^{-1} = 1 + k(\bar{M}_w(\text{i}))^{1/2} \quad (5)$$

which allows two problematic questions to be ignored: the choice of a suitable value for V_r and that of the appropriate average molecular weight.

Let us use now the experimental data with the aim to check directly eq 2. For this purpose, x_{PS} and x_{PVME} were deduced from the weight-average molecular weights of PS and PVME by considering V_r to be equal to the PVME repeat unit (Table III). In most blends under study, a discrepancy exists between the quantities $([(\phi_{PS})_{min}]^{-1} - 1)$ and $(x_{PS}/x_{PVME})^{1/2}$, so that a fit factor α must be introduced in eq 2, in agreement with Nishi's earlier data[4]

$$[(\phi_{PS})_{min}]^{-1} = 1 + \alpha(x_{PS}/x_{PVME})^{1/2} \quad (6)$$

The experimental error on α is large on account of the fact that small variations of $(\phi_{PS})_{min}$ may result in large variations on the quantity $([(\phi_{PS})_{min}]^{-1} - 1)$. It is the reason why α ranges are given in Table III instead of precise values. These α ranges were calculated on the assumption that the confidence ranges on w_{min} and both x_{PVME} and x_{PS} are 10% and 5%, respectively. Anyway, an unquestionable point is that the fit factor is significantly larger than unity in certain systems but close to one in some others. If the systems yielding $\alpha \gg 1$ might be used to question some of our assumptions (coincidence of the phase diagram minimum with the critical point, use of weight-average molecular weights), those corresponding to $\alpha \simeq 1$, on the other hand, give an account for their validity. As a matter of fact, the systems that exhibit the lowest α values result from the blending either of two high molecular weight polymers (lower part of Table III) or of two polymers containing low molecular weight chains (systems V99–S20 and V99–S35). In all other cases, α is larger than 3. Suppose that the calculated PS chain length is correct, this means that the effective PVME chain length would be a tenth of what it is actually. A crude explanation could be found in the presence of very short PVME chains in the polydisperse samples V45 and V99. The specific role of these chains would be to increase the compatibility of the longer ones with the PS chains. One may expect, indeed, such short chains to be numerous in samples V45 and V99 but few in samples V388, V633, and V1330. In other words, the dramatic deviations from the Scott equation ($\alpha > 3$) could result from a concentration dependence of the interaction coefficient, the profile of which may vary as a function of polymer molecular weights.

A final comment about the observed phase separation behavior deals with the values of $(T_{min})_\infty$, which were determined for three independent sets of blends in which the molecular weight of one component had been varied whereas that of the other one had been kept constant. Despite the fact that the invariant molecular weight differs from one set of systems to the other, the value of $(T_{min})_\infty$ remains the same, within the experimental error, whatever the set of blends under consideration (i.e., 97 ± 2 °C, as an average value from Table II). This independence with respect to the molecular weight of the second component suggests that $(T_{min})_\infty$ is an intrinsic characteristic of the pair PS–PVME. This finding agrees with the definition given by Nishi[4b]

$$(T_{min})_\infty = -B/AR \quad (7)$$

where R is the ideal gas constant and A and B are also

constants related to the temperature dependence of the interaction parameter χ between the two polymers

$$\chi = A + B/RT \quad (8)$$

Acknowledgment. We thank Dr. J. Lesec and M. Millequant at CNRS Paris (Laboratorie de Physicochimie Macromoléculaire) who provided us with the sample V45. The french authors acknowledge financial support from the Centre National de la Recherche Scientifique (Contract No. ATP 983 018).

Registry No. PS (homopolymer), 9003-53-6; PVME (homopolymer), 9003-09-2.

References and Notes

(1) Halary, J. L.; Ubrich, J. M.; Nunzi, J. M.; Monnerie, L.; Stein, R. S. *Polymer* **1984**, *25*, 956.
(2) (a) Halary, J. L.; Ubrich, J. M.; Monnerie, L.; Yang, H.; Stein, R. S. *Polym. Commun.* **1985**, *26*, 73. (b) Ben Cheikh Larbi, F.; Leloup, S.; Halary, J. L.; Monnerie, L. *Polym. Commun.* **1986**, *27*, 23.
(3) Nishi, T.; Kwei, T. K. *Polymer* **1975**, *16*, 285.
(4) (a) Nishi, T. *Rep. Prog. Polym. Phys. Jpn.* **1977**, *20*, 225. (b) Nishi, T. *J. Macromol. Sci., Phys.* **1980**, *B17*, 517.
(5) McMaster, L. P. *Macromolecules* **1973**, *6*, 760.
(6) Pincus, P. *J. Chem. Phys.* **1981**, *75*, 1996.
(7) Gelles, R.; Frank, C. W. *Macromolecules* **1983**, *16*, 1448.
(8) Scott, R. L. *J. Chem. Phys.* **1949**, *17*, 279.
(9) Brandrup, J.; Immergut, E. H. In "Polymer Handbook"; Wiley: New York, 1975; p 5-59.

Correlation between Ionic Conductivity and the Dynamic Mechanical Property of Polymer Complexes Formed by a Segmented Polyether Poly(urethane urea) and Lithium Perchlorate

Masayoshi Watanabe,* Kohei Sanui, and Naoya Ogata

Department of Chemistry, Sophia University, 7-1 Kioi-cho, Chiyoda-ku, Tokyo 102, Japan.
Received January 25, 1985

ABSTRACT: Ionic conductivity and the dynamic mechanical property were investigated in the polymer complexes formed by a segmented polyether poly(urethane urea) (PEUU), based on poly(propylene oxide) (PPO), and lithium perchlorate ($LiClO_4$). The PEUU formed a two-phase structure, consisting of the PPO and poly(urethane urea) phases, and $LiClO_4$ was selectively dissolved in the PPO phase. The frequency–temperature superposition for the storage elastic modulus was carried out in the temperature range for the backbone relaxation of the PPO segment, using the glass transition temperature (T_g) as a reference temperature. The ratios of the ionic conductivity at various temperatures (T) to that at T_g plotted againt $T - T_g$ were compared with the shift factors for the mechanical relaxation. The direct relationship between the ionic mobility and the local segmental motion of the PPO segment and the Arrhenius activation process for carrier generation were deduced from this comparison. A higher activation energy for the carrier generation was implied in the polymer complex containing $LiClO_4$ at a higher concentration.

Introduction

The studies on the ion-conducting behavior in certain kinds of ion-containing polymers are of considerable interest because these ion-containing polymers show relatively high ionic conductivity and are expected to be applicable to solid electrolytes in electrochemical devices.[1-10] Polyethers, such as poly(ethylene oxide)[1-5] and poly(propylene oxide) (PPO),[2,4-7] and polyesters, such as poly(β-propiolactone)[8] and poly(ethylene succinate),[9,10] have been selected as host polymers to alkali metal salts, and their ionic conductivity has been investigated. Glass transition temperatures (T_g) of these polymers lie below room temperature, and the conductivity data have been collected in their rubbery states. Therefore, it has been pointed out by several authors that transport of carrier ions correlates with the local segmental motion of these host polymers and obeys the free volume model[4,5,7] proposed by Cohen and Turnbull[11] or the configurational entropy model[12] proposed by Adam and Gibbs.[13] However, since conductivity is influenced not only by the carrier transport process but also by the carrier generation process, it is very difficult to analyze the conductivity data quantitatively, and only a few studies including the investigation of both carrier transport and generation processes have been carried out.[4,5,7]

We succeeded in a direct measurement of ionic mobility by the isothermal transient ionic current method,[7,14] which enabled the resolution of the conductivity into the ionic mobility and the number of carrier ions. The temperature dependence of the ionic mobility obeyed the free volume mechanism, whereas that of the number of carrier ions obeyed the Arrhenius activation mechanism. The quantitative equation that explains the temperature dependence of ionic conductivity in the rubbery state was, thus, derived from these results.[7] From the standpoint of the equation one can suppose the direct relationship between the ionic conductivity and the local segmental motion of the host polymers when the number of carrier ions is temperature-independent, in other words, when the incorporated salts dissociate completely.

Killis and Cheradame et al.[4,5,15] investigated the relationship between the dynamic mechanical property and ionic conductivity of the polyether networks containing sodium tetraphenylborate and showed that the ratios of the ionic conductivity at various temperatures to that at T_g directly correlated with the shift factors of the viscoelastic relaxation times. Furthermore, they showed[16] that the log–log plots of conductivity vs. salt concentration at constant reduced temperatures ($T - T_g$) were linear with slopes close to unity in the salt-containing poly(ethylene oxide) networks. They interpreted these results by assuming the complete dissociation of the incorporated salt.

In an earlier article,[17] we investigated the morphology and ionic conductivity of polymer complexes formed by segmented polyether poly(urethane urea) (PEUU), based on PPO, and lithium perchlorate ($LiClO_4$). PEUU formed

0024-9297/86/2219-0815$01.50/0